Journal of Computational Physics **161,** 700–717 (2000)
doi:10.1006/jcph.2000.6528, available online at http://www.idealibrary.com on IDEAL®

Modeling of Evanescent Energy in Optical Fibers

Gang Bao* and Tri Van†,[1]

**Department of Mathematics, Michigan State University, East Lansing, Michigan 48824; and †Department of Mathematics, University of Florida, Gainesville, Florida 32601*
E-mail: bao@math.msu.edu, Tri.Van@afit.af.mil

Received December 5, 1999; revised April 12, 2000

Optical fibers have found important applications in chemical imaging and single-particle detection. The applications make use of the propagating evanescent energy existing outside the core of a fiber. In this paper, a variational method is described to solve two-dimensional Helmholtz eigenvalue problems for a core of arbitrary shape. The method enables the problem in the infinite domain to be reduced to a bounded one by using a transparent boundary condition. It is shown that the variational formulation does not produce spurious solutions. An optimal error estimate is obtained for the associated finite element method. Finally, numerical experiments indicate that square fibers yield sufficient evanescent energy for imaging application.

Key Words: evanescent energy; finite element method; Helmholtz equation; transparent boundary condition.

1. INTRODUCTION

Optical fibers have been extensively used in telecommunications. Their high data-transmission rate is one of their most attractive features. This application mainly relies on the electromagnetic fields propagating inside the dielectric core of the fiber. The energy of these fields is concentrated in the core. The small portion of this energy existing just outside of the core surface, the so-called propagating evanescent energy, has recently found useful applications in single-particle detection and chemical imaging [4]. However, most of the research results available in the literature are for fibers with circular cores and are only concerned with the core-energy. For imaging purpose, evanescent energy is used and fibers with flat core surfaces, such as square fibers, are more convenient. This paper is devoted to the study of the propagating evanescent energy in non-circular fibers.

An optical fiber is oriented in $\mathbf{R}^3$ so that its longitudinal axis is parallel to the z-axis. Its geometry and materials are assumed to be independent of z. Thus, Maxwell's equations

[1] Current address: Air Force Institute of Technology, AFIT/ENC, Wright–Patterson AFB, Ohio 45433.

0021-9991/00 $35.00

can be reduced to two-dimensional Helmholtz eigenvalue equations defined in the infinite domain $\mathbf{R}^2$. For some fibers with circular core cross section, analytical solutions are possible, for example, step-index fibers and truncated parabolic fibers [14]. In general, one has to solve Helmholtz equations numerically. The standard finite element method of truncating the unbounded domain is often employed, by assuming that the fields vanish outside of a large but finite domain which consists of the core of the fiber. This truncation method not only is inaccurate but also yields spurious (non-physical) solutions [13]. In this paper, a finite element method is developed to reduce the computational efforts to a bounded domain and to eliminate spurious solutions by introducing a transparent boundary condition. This condition incorporates the exact solutions in the unbounded homogeneous region and the finite element solution in the bounded region containing the core of the fiber. This method is often used in scattering problems and exterior interface problems (see, for example, [7, 11] and references therein).

The paper is organized as follows. In Section 2, the two-dimensional Helmholtz equation governing the propagating transverse magnetic (TM) field is presented. In Section 3, an artificial boundary is introduced, which divides the original problem into two parts. One part is defined in a bounded region, the so-called interior problem, and the other is defined in the unbounded region, the so-called exterior problem. These sub-problems are coupled by an appropriate transparent boundary condition constructed on the artificial boundary using the field continuity conditions. In Section 4, the transparent boundary condition is used to reduce the eigenvalue problem defined in the infinite domain to an eigenvalue problem defined in a bounded domain, i.e., the interior problem. In Section 5, a variational formulation of the interior problem is given, which is the basis for the finite element method. Optimal convergence results for the finite element approximation are established. In Section 6, computational aspects of the method is discussed. Numerical experiments are presented to show the accuracy of the finite element approximation and comparisons of the evanescent energies in the square fibers and circular fibers are made. It is seen that square fibers can produce a significant amount of evanescent energy together with their flat core surface that can be very useful and convenient in molecule detection and imaging. The paper is concluded in Section 7.

2. HELMHOLTZ EQUATION FOR THE ELECTRIC FIELD

Let $\Omega \subset \mathbf{R}^2$ be the core region of the fiber and let $\Omega^c \equiv \mathbf{R}^2 \backslash \Omega$ be the cladding region. The refractive index distribution of the fiber is characterized by the function

$$n(x, y) = \begin{cases} n_1(x, y) & \text{in } \Omega \\ n_2 & \text{in } \Omega^c, \end{cases}$$

where $n_1(x, y)$ is a continuous function and $n_2 > 0$ is a constant. One can easily generalize the results of the paper to piecewise continuous functions n_1. For wave guidance taking place in the fiber, it is assumed that $n_2 < \max_{(x,y)\in\Omega} n_1(x, y) \equiv n_{\text{co}}$ throughout the paper.

Let $\mathbf{E}$ be the time-harmonic electric field (time dependence $e^{i\omega t}$). We wish to solve the time-harmonic Maxwell's equation for the electric field $\mathbf{E}(x, y) \in L^2(\mathbf{R}^2)$

$$\begin{aligned} \nabla \times \nabla \times \mathbf{E} &= k^2 n^2 \mathbf{E} \quad \text{in } \mathbf{R}^2, \\ \lim_{r\to\infty} r|\nabla \times \mathbf{E} - ik\mathbf{E}| &= 0, \quad r = \sqrt{x^2 + y^2}, \end{aligned} \tag{1}$$

where $k = 2\pi/\lambda$ is the wave number and λ is the wavelength. The tangential components of the solution $\mathbf{E}$ and of $\nabla \times \mathbf{E}$ are also required to be continuous at the interface of different materials.

DEFINITION 2.1. A *guided mode* $\mathbf{E}$ is a particular solution to (1) such that $\mathbf{E} \in L^2(\mathbf{R}^2)$ and is of the form

$$\mathbf{E} = Ee^{-i\beta z} = (E_x, E_y, E_z)e^{-i\beta z}, \tag{2}$$

where β is the propagation constant.

There are two fundamental cases of polarization, namely the transverse magnetic (TM) and the transverse electric (TE) polarization. In the TM case, the electric field $\mathbf{E}$ is parallel to the z axis ($E = (0, 0, E_z)$). In the TE case, the magnetic field $\mathbf{H}$ is parallel to the z axis ($H = (0, 0, H_z)$). In this paper, only TM polarization is considered. For the TE polarization, similar arguments and results can be used and obtained. For convenience, we denote $u = E_z$. Substituting (2) with $E_x = E_y = 0$ in (1), we obtain the Helmholtz eigenvalue equation defined in $\mathbf{R}^2$:

$$\text{(P)} \begin{cases} \text{Given } k, \text{ find all pairs } (\beta, u) \in (kn_2, kn_{\text{co}}) \times L^2(\mathbf{R}^2) \text{ such that} \\ \Delta u + (k^2 n^2 - \beta^2)u = 0 & \text{in } \Omega, \\ \Delta u + \left(k^2 n_2^2 - \beta^2\right)u = 0 & \text{in } \Omega^{\text{c}} \equiv \mathbf{R}^2 \backslash \Omega, \\ u(\mathbf{x}_0)^- = u(\mathbf{x}_0)^+ & \text{for } \mathbf{x}_0 \in \partial\Omega, \\ n(\mathbf{x}_0)\frac{\partial u}{\partial n}(\mathbf{x}_0)^- = n_2 \frac{\partial u}{\partial n}(\mathbf{x}_0)^+ & \text{for } \mathbf{x}_0 \in \partial\Omega, \\ \lim_{r\to\infty} r^{1/2}\left|\frac{\partial u}{\partial r} - iku\right| = 0, & \text{(radiation condition).} \end{cases}$$

The condition on the possible values of the propagation constants β's for guided modes is well-known (see for example [2]). Here, $\partial/\partial n$ denotes the differentiation of $\hat{n}$, the outward normal to $\partial\Omega$ and, for $\mathbf{x}_0 \in \partial\Omega$,

$$u(\mathbf{x}_0)^- \equiv \lim_{\substack{\mathbf{x}\to\mathbf{x}_0 \\ \mathbf{x}\in\Omega}} u(\mathbf{x}),$$
$$u(\mathbf{x}_0)^+ \equiv \lim_{\substack{\mathbf{x}\to\mathbf{x}_0 \\ \mathbf{x}\in\Omega^{\text{c}}}} u(\mathbf{x}).$$

We define $\partial u(\mathbf{x}_0)^{\pm}/\partial n$ in a similar fashion. The infinite nature of Problem (P) is the main difficulty in the computational viewpoint. By introducing a transparent boundary condition, one can reduce (P) to an eigenvalue problem over a bounded region of $\mathbf{R}^2$. In the next section, we construct the transparent boundary operator.

3. TRANSPARENT BOUNDARY CONDITION

Let B_R be a disc of radius $R > 0$ containing the core of the fiber Ω and let Γ_R be the boundary of B_R (see Fig. 1). Denote $u_{\text{i}} = u|_{B_R}$ and $u_{\text{e}} = u|_{B_R^{\text{c}}}$. We consider the auxiliary boundary value problem in the exterior region B_R^{c}:

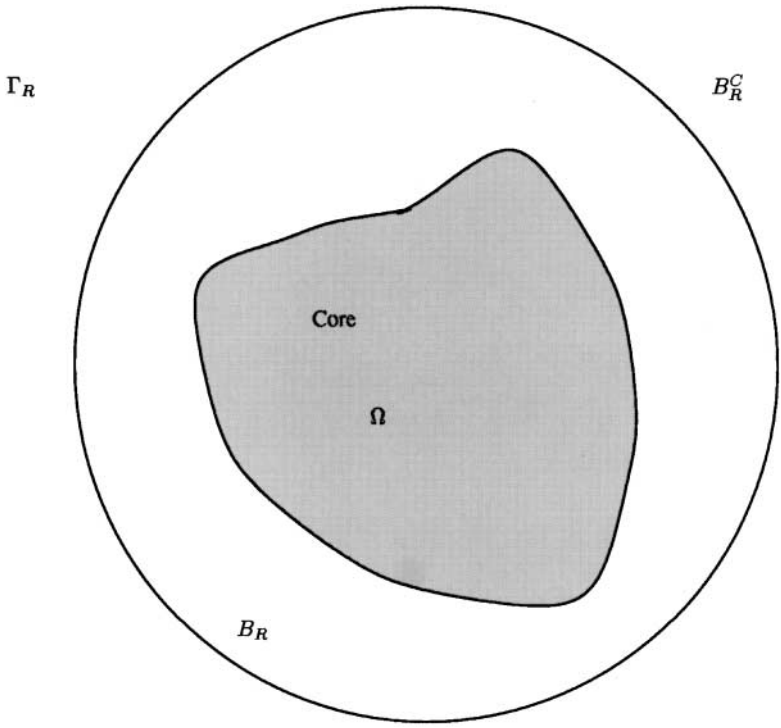

FIG. 1. Computational domain B_R and artificial boundary Γ_R.

$$(\mathrm{P_e})\begin{cases} \text{Let } g \in H^{1/2}(\Gamma_R) \quad \text{and} \quad \left(\beta^2 - k^2 n_2^2\right) > 0; \text{ find } u_\mathrm{e} \text{ such that} \\ \Delta u_\mathrm{e} - \left(\beta^2 - k^2 n_2^2\right) u_\mathrm{e} = 0 \quad \text{in } B_R^\mathrm{c}, \\ u_\mathrm{e} = g \quad \text{on } \Gamma_R, \\ \lim_{r\to\infty} r^{1/2} \left| \frac{\partial u_\mathrm{e}}{\partial n} - iku_\mathrm{e} \right| = 0. \end{cases}$$

It is well known in potential theory that the auxiliary problem $(\mathrm{P_e})$ has a unique solution $u_\mathrm{e} \in H^2(B_R^\mathrm{c})$ [8]. Hence, we can define the mapping

$$T_R : H^{1/2}(\Gamma_R) \to H^{-1/2}(\Gamma_R)$$
$$T_R[g](\mathbf{x}_0) \equiv \frac{\partial u_\mathrm{e}}{\partial n}(\mathbf{x}_0), \quad \mathbf{x}_0 \in \Gamma_R.$$

In fact, we can express T_R explicitly as follows. First, in polar coordinates, $(\mathrm{P_e})$ is written as

$$\frac{\partial^2 u_\mathrm{e}}{\partial r^2} + \frac{1}{r}\frac{\partial u_\mathrm{e}}{\partial r} + \frac{1}{r^2}\frac{\partial^2 u_\mathrm{e}}{\partial \theta^2} - \left(\beta^2 - k^2 n_2^2\right) u_\mathrm{e} = 0 \qquad \text{in } B_R^\mathrm{c},$$
$$u_\mathrm{e}|_{\Gamma_R} = g(\theta) \quad \text{on } \Gamma_R,$$
$$\lim_{r\to\infty} r^{1/2} \left| \frac{\partial u_\mathrm{e}}{\partial r} - iku_\mathrm{e} \right| = 0.$$

Using the Fourier series representation of u_e, i.e.,

$$u_\mathrm{e}(r,\theta) = \sum_{m=0}^{\infty} u_\mathrm{e}^{(m)}(r) e^{im\theta},$$

we obtain the modified Bessel equations, for $m = 1, 2, \ldots,$

$$\frac{d^2 u_e^{(m)}}{dr^2} + \frac{1}{r}\frac{du_e^{(m)}}{dr} - \left[\frac{m^2}{r^2} + \left(\beta^2 - k^2 n_2^2\right)\right] u_e^{(m)} = 0, \quad r > R.$$

Hence, for $r > R$,

$$u_e^{(m)}(r) = A_m K_m(\alpha r) + B_m I_m(\alpha r), \quad m = 0, 1, 2 \ldots,$$

where $\alpha = \sqrt{\beta^2 - k^2 n_2^2}$, A_m and B_m are constants, and K_m and I_m are modified Bessel functions of the second kind [1]. However, only $K_m(\alpha r)$ is an $L^2(B_R^c)$-function. Thus,

$$u_e(r, \theta) = \sum_{m=0}^{\infty} A_m K_m(\alpha r) e^{im\theta} \quad r \in (R, \infty), \theta \in [0, 2\pi).$$

On the boundary Γ_R, we also express the boundary function $g(\theta)$ in Fourier series, i.e.,

$$g(\theta) = \sum_{m=0}^{\infty} g^{(m)} e^{im\theta}.$$

Then, the condition $u_e = g$ on Γ_R yields

$$A_m K_m(\alpha R) = g^{(m)}, \quad m = 0, 1, 2, \ldots,$$

or

$$A_m = \frac{g^{(m)}}{K_m(\alpha R)}.$$

Therefore, the solution u_e is of the form

$$u_e(r, \theta) = \sum_{m=0}^{\infty} \frac{g^{(m)}}{K_m(\alpha R)} \cdot K_m(\alpha r) e^{im\theta}, \quad r \in (R, \infty), \theta \in [0, 2\pi),$$

and its normal derivative is

$$\left.\frac{\partial u_e}{\partial n}\right|_{\Gamma_R} = \left.\frac{\partial u_e}{\partial r}\right|_{\Gamma_R} = \sum_{m=0}^{\infty} \alpha \frac{K_m'(\alpha R)}{R_m(\alpha R)} g^{(m)} e^{im\theta}.$$

Now, we can explicitly define the mapping T_R as

DEFINITION 3.1. For each $g \in H^{1/2}(\Gamma_R)$, $T_R : H^{1/2}(\Gamma_R) \to H^{-1/2}(\Gamma_R)$ is defined by

$$\begin{aligned} T_R[g](\theta) &\equiv \sum_{m=0}^{\infty} \alpha \frac{K_m'(\alpha R)}{K_m(\alpha R)} g^{(m)} e^{im\theta} \\ &= \sum_{m=0}^{\infty} T_R^{(m)}[g] e^{im\theta}, \end{aligned}$$

where $\alpha = \sqrt{\beta^2 - k^2 n_2^2}$ and $T_R^{(m)}[g] = \alpha(K_m'(\alpha R)/K_m(\alpha R)) g^{(m)}$.

LEMMA 3.1. *$T_R : H^{1/2}(\Gamma_R) \to H^{-1/2}(\Gamma_R)$ is continuous.*

Proof. Let $\psi \in H^{1/2}(\Gamma_R)$; then

$$\begin{aligned}\langle T_R[\phi], \psi\rangle &\equiv \oint_{\Gamma_R} T_R[\phi]\cdot\bar{\psi}\, d\Gamma_R \\ &= \int_0^{2\pi}\left(\sum_{m=0}^{\infty} T_R^{(m)}[\phi]e^{im\theta}\cdot\sum_{m=0}^{\infty}\bar{\psi}^{(m)}\, e^{-im\theta}\right) R\, d\theta \\ &= 2\pi R\sum_{m=0}^{\infty} T_R^{(m)}[\phi]\bar{\psi}^{(m)} \\ &= 2\pi R\sum_{m=0}^{\infty}\alpha\frac{K_m'(\alpha R)}{K_m(\alpha R)}\phi^{(m)}\bar{\psi}^{(m)}.\end{aligned}$$

By the definition of dual norm, we have

$$\begin{aligned}\|T_R[\phi]\|_{H^{-1/2}(\Gamma_R)} &\equiv \sup_{\|\psi\|_{H^{1/2}(\Gamma_R)}=1} |\langle T_R[\phi], \psi\rangle| \\ &\le \sup_{\|\psi\|_{H^{1/2}(\Gamma_R)}=1} 2\pi R\sum_{m=0}^{\infty}\alpha\left|\frac{K_m'(\alpha R)}{K_m(\alpha R)}\right|\cdot\left|\phi^{(m)}\right|\cdot\left|\psi^{(m)}\right|.\end{aligned}$$

Since $K_m'(\alpha R) < 0$ and $k_m(\alpha R) > 0$, we can write

$$\left|\frac{K_m'(\alpha R)}{K_m(\alpha R)}\right| = \frac{-K_m'(\alpha R)}{K_m(\alpha R)}.$$

Using the following identity in [1]

$$zK_m'(z) = -mK_m(z) - zK_{m-1}(z),$$

we get

$$\frac{-K_m'(\alpha R)}{K_m(\alpha R)} = \frac{m}{\alpha R} + \frac{K_{m-1}(\alpha R)}{K_m(\alpha R)} \le \frac{m}{\alpha R} + 1.$$

Thus, since $0 < \alpha \le k\sqrt{n_{\text{co}}^2 - n_2^2}$, for sufficiently large n, we have

$$\alpha\left(\frac{m}{\alpha R} + 1\right) \le C(1+m^2)^{1/2},$$

where $C > 0$ is independent of α. Thus, for $m \gg 1$, we obtain

$$\sum_{m=0}^{\infty}\alpha\left|\frac{K_m'(\alpha R)}{K_m(\alpha R)}\right|\cdot\left|\phi^{(m)}\right|^2 \le C\sum_{m=0}^{\infty}(1+m^2)^{1/2}\cdot\left|\phi^{(m)}\right|^2.$$

Hence, by the Cauchy–Schwartz inequality, we obtain

$$\sum_{m=0}^{\infty}\alpha\left|\frac{K_m'(\alpha R)}{K_m(\alpha R)}\right|\cdot\left|\phi^{(m)}\right|\cdot\left|\psi^{(m)}\right| \le C\|\phi\|_{H^{1/2}(\Gamma_R)}.$$

So T_R is bounded in $H^{1/2}(\Gamma_R)$ as desired. ∎

4. INTERIOR PROBLEM

With the mapping T_R we can reduce the problem (P) to

$$\begin{cases} \text{Find } (\beta^2, u_i) \in \left(k^2 n_2^2, k^2 n_{\text{co}}^2\right) \times H^1(B_R)\backslash\{0\} \text{ such that} \\ \Delta u_{\text{i}} + (k^2 n^2 - \beta^2) u_{\text{i}} = 0 & \text{in } \Omega, \\ \Delta u_{\text{i}} + \left(k^2 n_2^2 - \beta^2\right) u_{\text{i}} = 0 & \text{in } B_R\backslash\Omega, \\ u_{\text{i}}(\mathbf{x}_0)^- = u_{\text{i}}(\mathbf{x}_0)^+ & \text{for } \mathbf{x}_0 \in \partial\Omega \\ n(\mathbf{x}_0) \frac{\partial u_{\text{i}}}{\partial n}(\mathbf{x}_0)^- = n_2 \frac{\partial u_{\text{i}}}{\partial n}(\mathbf{x}_0)^+ & \text{for } \mathbf{x}_0 \in \partial\Omega, \\ \frac{\partial u_{\text{i}}}{\partial n}\big|_{\Gamma_R} = T_R\left[u_{\text{i}}\big|_{\Gamma_R}\right] & \text{on } \Gamma_R. \end{cases}$$

We next show that the new problem (P_{i}) is equivalent to the original problem (P).

LEEMA 4.1. *The pair* $(\beta^2, u) \in (k^2 n_2^2, k^2 n_{\text{co}}^2) \times H^1(\mathbf{R}^2)\backslash\{0\}$ *is a solution of* (P) *iff* $(\beta^2, u_{\text{i}}) \in (k^2 n_2^2, k^2 n_{\text{co}}^2) \times H^1(\Omega)\backslash\{0\}$ *is a solution of the interior problem* (P_i).

Proof. Suppose (β^2, u) is a solution of (P). Denote $u_{\text{i}} \equiv u|_{B_R}$ and $u_{\text{e}} \equiv u|_{B_R^{\text{c}}}$. Then $u_i \neq 0$; otherwise, by the continuity conditions, $u_{\text{e}} = u_{\text{i}}$ and $\frac{\partial u_{\text{e}}}{\partial n} = \frac{\partial u_{\text{i}}}{\partial n}$ on Γ_R, we would get $u_{\text{e}}|_{\Gamma_R} = 0$ and $\frac{\partial u_{\text{e}}}{\partial n}|_{\Gamma_R} = 0$. This would imply that $u_{\text{e}} \equiv 0$, so $u \equiv 0$. By the definition of T_R, we see that

$$\begin{aligned} T_R\left[u_{\text{i}}\big|_{\Gamma_R}\right] &= T_R\left[u_{\text{e}}\big|_{\Gamma_R}\right] \\ &= \frac{\partial u_{\text{e}}}{\partial n}\bigg|_{\Gamma_R} \\ &= \frac{\partial u_{\text{i}}}{\partial n}\bigg|_{\Gamma_R}. \end{aligned}$$

Thus, $u|_{B_R}$ also satisfies the boundary condition in (P_{i}). Consequently, let (β^2, u_{i}) be a solution of (P_{i}).

Conversely, let u_{e} be the unique solution of the exterior problem with the boundary condition $u_{\text{e}}|_{\Gamma_R} = u_{\text{i}}|_{\Gamma_R}$. Hence, we see that

$$\frac{\partial u_{\text{i}}}{\partial n}\bigg|_{\Gamma_R} = T_R\left[u_{\text{i}}\big|_{\Gamma_R}\right] = T_R\left[u_{\text{e}}\big|_{\Gamma_R}\right] = \frac{\partial u_{\text{e}}}{\partial n}\bigg|_{\Gamma_R}.$$

Thus, $u_{\text{e}}|_{\Gamma_R} = u_{\text{i}}|_{\Gamma_R}$ and $\frac{\partial u_{\text{e}}}{\partial n}|_{\Gamma_R} = \frac{\partial u_{\text{i}}}{\partial n}|_{\Gamma_R}$ are satisfied. The function u whose restrictions on B_R and B_R^{c} are u_{i} and u_{e} is a solution of (P). The uniqueness of u follows from the uniqueness of u_{e} and the unique continuation theorem for Δ operator [9]. ∎

The reduced problem (P_{i}) can be solved by variational methods.

5. VARIATIONAL FORMULATION OF THE INTERIOR PROBLEM

Let $H = L^2(B_R)$ with the usual inner product. We define the space

$$V \equiv \left\{v \in H^1(B_R) : v(\mathbf{x}_0)^- = v(\mathbf{x}_0)^+, \mathbf{x}_0 \in \partial\Omega\right\} \subset H$$

with norm

$$|||v|||_1 \equiv \|v\|_{1,B_R} + \|v\|_{1,B_R^{\text{c}}}.$$

We also define $|||v|||_0 \equiv \|v\|_{0,B_R} + \|v\|_{0,B_R^{\text{c}}}$ Clearly, V is a Hilbert space with norm $|||\cdot|||_1$.

Let n_α be an arbitrary constant such that $n_\alpha > n_{\mathrm{co}}$. We define the bilinear form $b(\cdot,\cdot)$ in $V \times V$ as

$$\begin{aligned} b(u,u) &= \int_{B_R} \nabla u \cdot \nabla \bar{v}\, dx\, dy + k^2 \int_{B_R} \left(n_\alpha^2 - n^2\right) u \bar{v}\, dx\, dy - \oint_{\Gamma_R} T_R\left[u\big|_{\Gamma_R}\right] \bar{v}\, dS \\ &= \int_{B_R} \nabla u \cdot \nabla \bar{v}\, dx\, dy + k^2 \int_{B_R} \left(n_\alpha^2 - n^2\right) u \bar{v}\, dx\, dy \\ &\quad + 2\pi R \sum_{m=0}^{\infty} (-\alpha) \frac{K_m'(\alpha R)}{K_m(\alpha R)} u^{(m)} \bar{v}^{(m)}. \end{aligned}$$

Note that we have introduced the term $k^2 n_\alpha^2(u, v)$ into the variational form.

THEOREM 5.1. *For each $f \in L^2(B_r)$, there is a unique solution $u \in V$ to the non-homogeneous variational equation*

$$b(u, v) = (f, v) \quad \forall v \in V. \tag{3}$$

Proof. The existence and uniqueness of the solution $u \in V$ is the standard consequence of the Lax–Milgram lemma. In fact, we show that the bilinear form $b(\cdot,\cdot)$ is bounded and coercive in $V \times V$. Since the linear map T_R is bounded in $H^{-1/2}(\Gamma_R)$, we have

$$\left\| T_R\left(u\big|_{\Gamma_R}\right) \right\|_{H^{-1/2}(\Gamma_R)} \le C \|u\|_{H^{1/2}(\Gamma_R)}.$$

Hence, by Schwartz's inequality, we have

$$\begin{aligned} \left| \oint_{\Gamma_R} T_R\left(u\big|_{\Gamma_R}\right) \bar{v}\, d\Gamma_R \right| &\le C \|u\|_{H^{1/2}(\Gamma_R)} \|v\|_{H^{1/2}(\Gamma_R)} \\ &\le C |||u|||_1 |||v|||. \end{aligned}$$

The last inequality follows from the trace theorem. Thus, we have

$$\begin{aligned} |b(u,v)| &\le \|\nabla u\|_{0,B_R} \|\nabla v\|_{0,B_R} + k^2 \left(n_\alpha^2 - n_2^2\right) \|u\|_{0,B_R} \|v\|_{0,B_R} + C |||v|||_1 |||v|||_1 \\ &\le C |||u|||_1 |||v|||_1. \end{aligned}$$

Hence, $b(u, v)$ is bounded in $V \times V$. To show that $b(\cdot,\cdot) > 0$, we notice that $-\frac{K_n'(\alpha R)}{K_n(\alpha R)} > 0$; we get

$$b(u,u) \ge \|\nabla u\|_{0,B_R}^2 + k^2 \left(n_\alpha^2 - n^2\right) \|u\|_{0,B_R}^2 \ge C |||v|||_1^2.$$

Thus, $b(\cdot,\cdot) > 0$ for non-zero $u \in V$. This completes the proof. ∎

By a representation theorem for bounded symmetric bilinear forms, there exists a unique bounded self-adjoint operator B defined on $D(B) \subset V$ such that

$$b(u, v) = (Bu, v) \quad \forall u, v \in V,$$

and B has the same bounds as $b(\cdot,\cdot)$. Since 0 is a point in the resolvent set of B, the resolvent $T \equiv B^{-1}$ is well defined, i.e., T is bounded.

LEMMA 5.1. *T is compact in H.*

Proof. Since $H^1(\Omega)$ is compactly embedded in $H = L^2(\Omega)$, T is bounded and V is closed in H,

$$T : H \to D(B) \subset V \subset H^1(\Omega) \hookrightarrow H$$

is compact. ■

This implies that

THEOREM 5.2 [10]. *The spectrum of B consists entirely isolated eigenvalues with finite multiplicities and $R_\zeta(B) \equiv (B - \zeta I)^{-1}$ is compact for every ζ in the resolvent set of B.*

5.1. *Finite Element Approximation*

Let $\{V_h : h \in (0, 1)\}$ be a family of finite dimensional subspaces of V, which satisfy the approximation property

Approximation property. There exist an integer $s \geq 2$ and positive constants C_0 and C_1 such that for any $v \in V$ with $|||v|||_l < \infty$, $l \leq s$, there exists a function $\varphi \in V_h$ such that

$$|||v - \varphi|||_j \leq C_j h^{l-j} |||v|||_s, \quad j = 0, 1.$$

For simplicity, we choose the approximation spaces $\{V_h\}$ as sets of continuous piecewise linear functions in B_R. Consider the non-homogeneous problem associated with (P)

$$\text{(NP)} \begin{cases} \text{Let } f \in H^{l-2}(\mathbf{R}^2), l \geq 2; \text{ find } u \text{ such that} \\ \Delta u + (k^2 n^2 - \beta^2) u = f|_\Omega & \text{in } \Omega, \\ \Delta u + \left(k^2 n_2^2 - \beta^2\right) u = f|_{\Omega^c} & \text{in } \Omega^c, \\ u(\mathbf{x}_0)^- = u(\mathbf{x}_0)^+ & \text{for } \mathbf{x}_0 \in \partial\Omega, \\ n(\mathbf{x}_0) \frac{\partial u}{\partial n}(\mathbf{x}_0)^- = n_2 \frac{\partial u}{\partial n}(\mathbf{x}_0)^+ & \text{for } \mathbf{x}_0 \in \partial\Omega, \\ \lim_{r \to \infty} r^{1/2} \left| \frac{\partial u}{\partial r} - iku \right| = 0, & \text{(radiation condition).} \end{cases}$$

The regularity results for the solution of the non-homogeneous problem (NP) imply that $u|_\Omega \in H^l(\Omega)$ and $u|_{B_R \setminus \Omega} \in H^l(B_R \setminus \Omega)$. Hence, in particular, if $f \in L^2(\mathbf{R}^2)$, the family of continuous linear functions $\{V_h\}$ satisfies the approximation property for $s = 2$ [3].

In analyzing error estimates, we also consider the discrete non-homogeneous problem

$$\text{let } f \in H; \text{ find } u_h \in V_h \text{ such that}$$
$$b(u_h, v_h) = (f, v_h) \quad \forall v_h \in V_h.$$

Let $(B_h, D(B_h))$ be the unique self-adjoint operator associated to $b(\cdot, \cdot) : V_h \times V_h \to \mathbb{C}$. Let $T_h \equiv B_h^{-1}$. Then T_h is compact; in fact, T_h is of finite rank. Then a unique solution u_h to the non-homogeneous problem is of the form

$$u_h = T_h f, \quad f \in H.$$

THEOREM 5.3. *Let u be a unique solution of the variational problem*

$$b(u, v) = (f, v), \quad v \in V. \tag{4}$$

Then there exists $h_0 > 0$ such that the solution u_h, $0 < h < h_0$, of

$$b(u_h, v_h) = (f, v_h), \quad v_h \in V_h,$$

satisfies

$$|||u - v_h|||_0 \le C_0 h |||u - v_h|||_1, \quad |||u - u_h|||_1 \le C_1 h.$$

Proof. Let $f \in H$. Let u be the solution of $b(u, v) = (f, v)$, $v \in V$. By Céa's lemma [3] and the approximation property of V_h, we have

$$\begin{aligned} b(u - u_h, u - \tilde{u}_h)^{1/2} &\le C_1 \inf_{v_h \in V_h} b(u - v_h, u - v_h)^{1/2} \\ &\le C_1 \inf_{v_h \in V_h} |||u - v_h|||_1 \\ &\le C_1 h. \end{aligned} \tag{5}$$

But we also have the coercivity of the bilinear form $b(\cdot, \cdot)$

$$b(u - u_h, u - u_h)^{1/2} \ge C_1 |||u - u_h|||_1; \tag{6}$$

thus by combining (4) and (6), we obtain

$$|||u - u_h|||_1 \le C_1 h.$$

This shows the second inequality in the theorem. To show the first inequality, we apply *Nitsche's technique* [6] as follows. Let $g \in H$, $\|g\|_0 = 1$. Let $w_g \in V$ be the unique (dual) solution of

$$b(v, w_g) = (g, v), \quad v \in V.$$

Let φ be an arbitrary element of V_h; then

$$\begin{aligned} \inf_{w_h \in V_h} b(w_g - w_h, w_g - w_h)^{1/2} &\le C_0 b(w_g - \varphi, w_g - \varphi)^{1/2} \\ &\le C_0 |||w_g - \varphi|||_1. \end{aligned}$$

Therefore, $|||w_g - w_h|||_1 \le C_0 h$ by the approximation property of V_h. Thus, by the *Aubin–Nitsche Lemma* [3], we get

$$\begin{aligned} \|u - u_h\|_0 &\le C_0 |||u - u_h|||_1 \left(\sup_{\|g\|_{L^2(\Omega)} = 1} \inf_{w_h \in V_h} |||w_g - w_h|||_1 \right) \\ &\le C_0 h |||u - u_h|||_1. \end{aligned}$$

This proves the first inequality. ∎

COROLLARY 5.1. *For $h > 0$ sufficiently small, we have*

$$\|T_h - T\| \le Ch.$$

Remark. This corollary implies that the compact discrete operators T_h converges in norm to the compact operator T. Hence, the (discrete) spectrum of T_h also converges to the (discrete) spectrum of T [10]. As a result, no spurious eigenvalues exist.

Now we consider the variational form of eigenvalue problem,

$$\begin{aligned} &\text{find } (\lambda, u) \in \left(0, k^2 n_\alpha^2 - k^2 n_{\text{cl}}\right) \times V \text{ such that} \\ &\quad b(u, v) = \lambda(u, v) \quad \forall v \in V, \end{aligned}$$

where $\lambda = k^2 n_\alpha^2 - \beta^2$. By Theorem 5.2 the eigenvalues λ are isolated since if μ is an eigenvalue of T then $\lambda = \frac{1}{\mu}$. This is important for numerical computations. The associated discrete eigenvalue problem is

$$\begin{aligned} &\text{find } (\lambda_h, u_h) \in \left(0, k^2 n_\alpha^2 - k^2 n_{\text{cl}}\right) \times V_h \text{ such that} \\ &\quad b(u_h, v_h) = \lambda_h(u_h, v_h) \quad \forall v_h \in V_h. \end{aligned}$$

We now state the standard theorem in finite element theory on the convergence rate of the eigenvalues and eigenvectors for the operator B with compact resolvent T.

THEOREM 5.4. *[5] Let λ_0 be an isolated eigenvalue of B with a normalized eigenvector u_0. Then there exists an eigenvalue λ_h of B_h with a normalized eigenvector u_h such that*

$$|\lambda_h - \lambda_0| \le Ch^2$$

and

$$\|u_h - u_0\|_0 \le Ch.$$

6. COMPUTATION

In this section, we discuss the implementation of the presented finite element method and illustrate the accurary of the numerical results. For each given k, we consider the eigenvalue problem

$$b(u, v) = \lambda(u, v), \quad \forall v \in V \tag{7}$$

where $\lambda = k^2 n_\alpha^2 - \beta^2$, $n_\alpha > \max_{B_R} n(x, y)$ and

$$b(u, v) = \int_\Omega \nabla u \nabla v \, dx \, dy + \int_\Omega k^2 \left(n_\alpha^2 - n^2\right) uv \, dx \, dy - \oint_{\Gamma_R} T_R uv \, d\Gamma_R$$

with

$$T_R u = \sum_{m=0}^{\infty} \alpha \frac{K_m'(\alpha R)}{K_m(\alpha R)} u^{(m)} e^{im\theta}, \quad \alpha = \sqrt{\beta^2 - k^2 n_2^2}.$$

For computation, we rewrite the series expansion of the boundary operator T_R as

$$T_R u = \sum_{m=0}^{\infty} \alpha \frac{K_m'(\alpha R)}{K_m(\alpha R)} \left(u_1^{(m)}(R) \cos(m\theta) + u_2^{(m)}(R) \sin(m\theta)\right),$$

where $u_1^{(m)}(r)$ and $u_2^{(m)}(r)$ are the Fourier coefficients of u defined as

$$u_1^{(0)}(r) = \frac{1}{2\pi}\int_0^{2\pi} u(r,\theta)\,d\theta,$$
$$u_1^{(m)}(r) = \frac{1}{\pi}\int_0^{2\pi} u(r,\theta)\cos(m\theta)\,d\theta, \quad \text{for } m \geq 1,$$
$$u_2^{(0)}(r) = 0,$$
$$u_2^{(m)}(r) = \frac{1}{\pi}\int_0^{2\pi} u(r,\theta)\sin(m\theta)\,d\theta, \quad \text{for } m \geq 1.$$

6.1. *Discretized Non-linear Eigenvalue Problem*

We define a triangulation $\mathcal{T}$ in the bounded computational domain B_R such that the corresponding partition $\mathcal{P}$ of the circle Γ_R is equally spaced. Let V_h be the finite dimensional subspace of V consisting of continuous piecewise linear functions in B_R,

$$V_h \equiv \left\{v_h \in V : v_h|_\tau \in P^1(\tau),\, \tau \in \mathcal{T},\, v_h|_\gamma \in P^1(\gamma),\, \gamma \in \mathcal{P}\right\}.$$

V_h satisfies the approximation property [3]. In each triangle $\tau \in \mathcal{T}$, we denote the nodal basis functions as $N_j^\tau(x,y)$, $j = 1, 2, 3$. Hence, the approximate solution $u_h \in V_h$ can be expressed as

$$u_h(x,y) = \sum_{\tau\in\mathcal{T}}\sum_{j=1}^{3} U_j^\tau N_j^\tau(x,y) \tag{8}$$

where U_j^τ is the value of u_h at the jth vertex of the triangle τ. Substituting (8) into the variational problem (7), we obtain the non-linear eigenvalue equation

$$[A - M(\beta)]U = \lambda(\beta)BU, \quad \lambda(\beta) = k^2 n_\alpha^2 - \beta^2, \tag{9}$$

where

$$A = \sum_\tau [A^\tau] = \sum_\tau (A^\tau)_{ij}, \quad i, j = 1, 2, 3,$$
$$B = \sum_\tau [B^\tau] = \sum_\tau (B^\tau)_{ij}, \quad i, j = 1, 2, 3,$$
$$M(\beta) = \sum_\gamma [M^\gamma(\beta)] = \sum_\gamma (M^\gamma(\beta))_{kl}, \quad k, l = 1, 2,$$

with

$$(A^\tau)_{ij} = \int_\tau \left[\nabla N_i^\tau \cdot \nabla N_j^\tau + k^2\left(n_\alpha^2 - n^2\right) N_i^\tau N_j^\tau\right] dx\,dy,$$
$$(B^\tau)_{ij} = \int_\tau N_i^\tau N_j^\tau\,dx\,dy, \quad N_i^\tau(x,y), N_i^\tau(x,y) \in P^1(\tau),$$
$$(M(\beta)^\gamma)_{\boldsymbol{kl}} = \int_0^{2\pi} T_R\left[N_k^\gamma\right] N_l^\gamma\,d\theta,$$
$$= \sum_{m=0}^{\infty} \alpha \frac{K_n'(\alpha R)}{K_n(\alpha R)}\left[\left(N_k^\gamma\right)_1^{(m)}\left(\boldsymbol{N}_l^\gamma\right)_1^{(m)} + \left(N_k^\gamma\right)_2^{(m)}\left(N_l^\gamma\right)_2^{(m)}\right.,$$
$$N_k^\gamma(\theta), N_l^\gamma(\theta) \in P^1(\gamma).$$

The terms $(N_k^\gamma)_1^{(m)}$ and $(N_k^\gamma)_2^{(m)}$ are the cosine and sine Fourier coefficients, respectively, of the linear function $N_k^\gamma(\theta)$. To compute the discrete eigenvalues and their corresponding eigenvectors of the non-linear eigenvalue problem, we view it as a fixed-point problem

$$\lambda(\beta) - \left(k^2 n_\alpha^2 - \beta^2\right) = 0, \quad kn_0 < \beta < kn_{\text{co}}$$

which can be solved numerically by the secant method. During the secant algorithm, one needs to solve the generalized (linear) eigenvalue problem

$$\text{given } \beta, \text{ find } \lambda \text{ and } U \text{ in}$$
$$[A - M(\beta)]U = \lambda BU,$$

where B is symmetric and positive definite. In this paper, we employ the approach given in ([12, p. 455]),

6.2. *Evanescent Energy*

For each eigenvalue β, the energy of the corresponding propagating mode u is computed as follows. As before, let u_{e} be the restriction of u to the exterior domain B_R^{c} and let u_{i} be the restriction of u to the interior domain B_R. We define the energy of u as

$$\begin{aligned}\mathcal{E}(u) &\equiv |||u|||_1 \\ &= \int_{B_R} (|u_{\text{i}}|^2 + |\nabla u_{\text{i}}|^2)\, dx\, dy + \int_{B_R^{\text{c}}} (|u_{\text{e}}|^2 + |\nabla u_{\text{e}}|^2)\, dx\, dy \\ &= \int_{B_R} |u_{\text{i}}|^2\, dx\, dy + \int_{B_R^{\text{c}}} |u_{\text{e}}|^2\, dx\, dy + \int_{\mathbf{R}^2} |\nabla u|^2\, dx\, dy.\end{aligned}$$

The percentage of the evanescent energy existing outside the core Ω is

$$\mathcal{E}_{\text{e}} = 1 - \frac{\mathcal{E}(u|_\Omega)}{\mathcal{E}(u)}. \tag{10}$$

We now briefly discuss the computation of $\mathcal{E}_{\text{e}}$. First, $\mathcal{E}(u|_\Omega)$ and $\|u_{\text{i}}\|^2_{L^2(B_R)}$ can be easily computed by a 2D numerical quadrature on the triangular mesh. To compute $\|u_{\text{e}}\|^2_{B_R^{\text{c}}}$ we recall that u_{e} satisfies

$$u_{\text{e}}(r,\theta) = \sum_{m=0}^{\infty} \frac{K_m(\alpha r)}{K_m(\alpha R)} \left[u_{i,1}^{(m)} \cos(m\theta) + u_{i,2}^{(m)} \sin(m\theta)\right],$$

where $u_{i,1}^{(m)}$ and $u_{i,2}^{(m)}$ are the cosine and sine coefficients of the Fourier series representation of $u_{\text{i}}(R,\theta)$, respectively. Using the identity [14]

$$\int K_m^2(az) z\, dz = \frac{z^2}{2}\left[K_m^2(az) - K_{m+1}(az) K_{m-1}(az)\right]$$

we have

$$\begin{aligned}\int_{B_R^{\text{c}}} |u_{\text{e}}|^2\, dx\, dy &= \int_0^{2\pi} \int_R^{\infty} |u_{\text{e}}(r,\theta)|^2 r\, dr\, d\theta \\ &= \pi \frac{R^2}{K_m^2(\alpha R)} \sum_{m=0}^{\infty} \left(u_{i,1}^{(m)^2} + u_{i,2}^{(m)^2}\right)\left[K_{m+1}(\alpha R) K_{m-1}(\alpha R) - K_m^2(\alpha R)\right]. \end{aligned} \tag{11}$$

Finally, we note that the solution pair (β, u) satisfies the variational equation

$$\int_{\mathbf{R}^2} |\nabla u|^2 \, dx\, dy = \int_{\mathbf{R}^2} (k^2 n^2 - \beta^2)|u|^2 \, dx\, dy$$
$$= \int_{B_R} (k^2 n^2 - \beta^2)|u_{\mathrm{i}}|^2 \, dx\, dy + \left(k^2 n_2^2 - \beta^2\right) \int_{B_R^{\mathrm{c}}} |u_{\mathrm{e}}|^2 \, dx\, dy.$$

The last term in the above equation can be computed using (11).

6.3. *An Example*

We now present an example to study the accuracy of the method. Consider a step-index circular fiber with core radius $a = 1$, core refractive index $n_{\mathrm{co}}^2 = 2$, and cladding index $n_2^2 = 1$. Let Γ_R be a circle of radius $R = 2$. For the circular case, there exist exact analytical solutions. In fact, (P) can be expressed in polar coordinates as

$$\begin{cases} \frac{\partial^2 E_z}{\partial r^2} + \frac{1}{r}\frac{\partial E_z}{\partial r} + \frac{1}{r^2}\frac{\partial^2 E_z}{\partial \theta^2} + \left(k^2 n_{\mathrm{co}}^2 - \beta^2\right) E_z = 0 & r \le a, \\ \frac{\partial^2 E_z}{\partial r^2} + \frac{1}{r}\frac{\partial E_z}{\partial r} + \frac{1}{r^2}\frac{\partial^2 E_z}{\partial \theta^2} + \left(k^2 n_2^2 - \beta^2\right) E_z = 0 & r > a. \end{cases}$$

By separation of variables, E_z can be written as

$$E_z = \sum_m F_m(r)\Phi_m(\theta) e^{-i\beta_m z}$$

where each $F_m(r)$ is a solution of

$$\frac{d^2 F_m}{dr^2} + \frac{1}{r}\frac{dF_m}{dr} + \left(k^2 n^2 - \frac{m^2}{r^2}\right) = 0, \quad r \in \mathbf{R}, \tag{12}$$

and $\Phi(\theta)$ is a solution of

$$\frac{d^2 \Phi_m}{d\theta^2} + m^2 \Phi = 0, \quad \theta \in [0, 2\pi).$$

Equation (12) is a form of Bessel's equations. Thus, its solutions are of the form

$$F_m(r) = \begin{cases} A_m J_m(Ur/a) & \text{for } r \le a, \\ B_m K_m(Wr/a) & \text{for } r > a, \end{cases} \tag{13}$$

where J_m and K_m are Bessel functions and modified Bessel functions, respectively, and

$$U = a\sqrt{k^2 n_{\mathrm{co}}^2 - \beta^2}, \quad W = a\sqrt{\beta^2 - k^2 n_2^2}.$$

We normalize solutions (13) at the core-cladding interface as $J_m(Ur/a)/J_m(U)$ and $K_m(Wr/a)/K_m(W)$. Applying the continuity condition of the normal derivatives at the

TABLE 1
Convergence of the FEM Eigenvalue for $k^2 = 3.76263$

N vertices	h	β_h (FEM eigenvalue)[a]	$\lvert\beta_{h/2} - \beta_h\rvert$ (convergence error)
49	.7789	2.19906	
169	.4203	2.24219	$2.24219 - 2.19906 = .0431$
625	.2219	2.25213	$2.25213 - 2.24219 = .0099$
2401	.1137	2.25430	$2.25430 - 2.25213 = .0022$

Note. The fiber is a step-index circular fiber with

$$n^2(x, y) = \begin{cases} 2 & r \le 1 \\ 1 & r > 1. \end{cases}$$

The artificial boundary Γ_R is the circle of radius 2.
[a] Computed by (10).

interface to the normalized field, we get the "exact" eigenvalue equations for a step-index fiber

$$U\frac{J_m'(U)}{J_m(U)} = W\frac{K_m'(W)}{K_m(W)} \quad m = 0, 1, 2, \ldots. \tag{14}$$

Therefore, we can study the accuracy of the finite element method by comparing its eigenvalues to the "exact" ones found by (14). Let $k^2 = 3.76263$ and $k^2 = 4.32158$. The corresponding exact eigenvalues are $\beta = 2.2920$ ($m = 0$) and $\beta = 2.4956$ ($m = 0$), respectively. The eigenvalues β computed by the finite element method (9) for different mesh size h (the longest edge of the triangular elements) are listed in Table 1 and Table 2. One sees that the convergence is of order 4 for β and hence of order 2 for $\lambda = \beta^2$ as predicted by the theory.

Finally, we consider a step-index square fiber which has the same cross section area as that of the step-index circular fiber considered in the above example. We also assume that the core index of the square fiber is the same as that of the circular fiber, that is, $n_{\text{co}}^2 = 2$. We wish to compare their evanescent energy. Thus, the considering square fiber

TABLE 2
Convergence of the FEM Eigenvalue for $k^2 = 4.32158$

N vertices	h	β_h (FEM eigenvalue)[a]	$\lvert\beta_{h/2} - \beta_h\rvert$ (convergence error)
49	.7789	2.41035	
169	.4203	2.45582	$2.45582 - 2.41035 = .0455$
625	.2219	2.46642	$2.46642 - 2.45582 = .0106$
2401	.1137	2.46883	$2.46883 - 2.46642 = .0024$

Note. The fiber is a step-index circular fiber with

$$n^2(x, y) = \begin{cases} 2 & r \le 1 \\ 1 & r > 1. \end{cases}$$

The artificial boundary Γ_R is the circle of radius 2.
[a] Computed by (10).

TABLE 3
Comparison of the Percentage of Evanescent Energy $\mathcal{E}_e^a$ in the Circular and Square Fibers for different k^2

k^2	$\mathcal{E}_e$ of circular fiber[b]	$\mathcal{E}_e$ of square fiber[b]
3.762625	25%	37%
4.321575	23%	35%
4.883703	21%	33%
5.783529	20%	32%
6.526149	19%	31%

[a] Computed by (11).
[b] The fibers have the same core area and

$$n^2(x, y) = \begin{cases} 2 & \text{in } \Omega \text{ (circular or square core)} \\ 1 & \text{otherwise.} \end{cases}$$

has dimension $\sqrt{\pi} \times \sqrt{\pi}$. The computational domain for both fibers is the same as before, that is, $\{\mathbf{x} : |\mathbf{x}| \leq 2\}$. The evanescent energy of each mode excited in a fiber is computed by (10). We vary the wave number k and observe the change in the evanescent energy in each fiber. Since the lower order modes are dominant, we concentrate on the fundamental propagating mode (which corresponds to the solution to (12) for $m = 0$). In Table 3, we computed the percentage of energy existing outside of the core for each fiber as a function of k. We observe that as the wave number k decrease, more evanescent energy exists outside of each fiber. Moreover, the evanescent energy of the square fiber is greater than that of the circular fiber. This suggests that square fibers can be effectively used in molecule detection and chemical imaging. For completeness, the total intensity $|E_z|$ of each fiber and its cladding intensity in the computational domain is plotted for $k^2 = 4.321575$ in Fig. 2A (for the circular fiber) and Fig. 2B (for the square fiber).

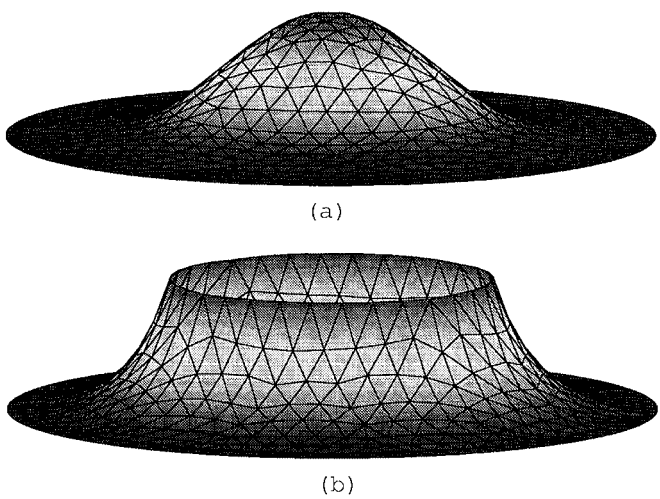

FIG. 2A. Circular fiber: the intensity distribution of the fundamental mode (a) in the computational domain B_R, $R = 2$, and its evanescent portion (b) (not to scale) in $B_R \backslash \Omega$, where Ω is the fiber core.

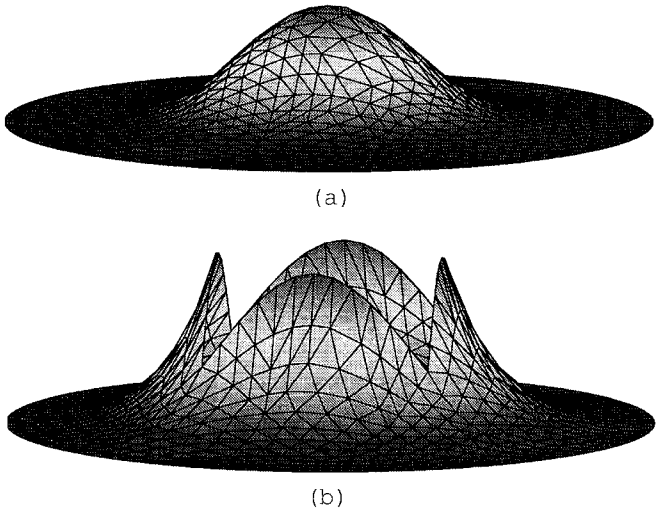

FIG. 2B. Square fiber: the intensity distribution of the fundamental mode (a) in the computational domain B_R, $R = 2$, and its evanescent portion (b) (not to scale) in $B_R \backslash \Omega$ where Ω is the fiber core.

7. CONCLUSION

We have constructed a transparent boundary condition which reduces the computational efforts of the eigenvalue Helmholtz equation defined in the infinite domain to an interior problem defined in a bounded domain. The finite element method based on the variational formulation of the reduced problem is shown to have no spurious solutions and the optimal convergence results are obtained. The accuracy of the method has been demonstrated through comparisons to the available exact eigenvalues. Furthermore, the numerical experiments indicate that propagating evanescent energy in a plastic squre fiber is sufficiently strong to be useful in imaging applications.

ACKNOWLEDGMENT

This work was partially supported by NSF Grant DMS 98-03634, the NSF University-Industry Cooperative Research Programs Grants DMS 98-03809, DMS 99-72292, Office of Naval Research (ONR) Grant N0001 40010299, and NSF Western Europe Programs Grant INT 98-15798. We thank Dr. Weihong Tan and Dr. Xiaohong Fang at the Department of Chemistry, University of Florida, for helpful discussions.

REFERENCES

1. M. Abramowitz and I. A. Stegun, *Handbook of Muthematical Functions* (Dover, New York, 1965).
2. J. Buck, *Fundamentals of Optical Fibers* (Wiley, New York, 1995).
3. P. Ciarlet, *The Finite Element Method for Elliptic Problems* (North-Holland, Amsterdam, 1978).
4. , X. Fang and W. Tan, Imaging single fluorescentmolecules at the interface of an optical fiber probe by evanescent wave excitation, *Anal. Chem.* **71**, 3101–3105 (1999).
5. G. Fix, Eigenvalue approximation by the finite element method, *Advances in Math.* **10**, 300–316 (1973).
6. G. Fix and G. Strang, *An Analysis of The Finite Element Method* (Prentice Hall, Englewood Cliffs, 1973).
7. D. Givoli, *Numerical Methods for Problems in Infinite Domains* (Elsevier, Amsterdam, 1992).
8. G. Hsiao and R. C. MacCamy, Solution of boundary value problems by integal equations of the first kind, *SIAM Rev.* **15**, No. 4, 687 (1963).

9. L. Hörmander, *Uniqueness Theorems for Second Order Elliptic Differential Equations, Commu. Partial Differential Equations* **8**, 21 (1983).
10. T. Kato, *Perturbation Theory for Linear Operators* (Springer-Verlag, New York, 1976).
11. R. C. MacCamy and S. P. Marin, A finite element method for exterior interface problems, *Internat. J. Math. Math. Sci.* **3**, No. 2, 311 (1980).
12. W. H. Press, S. A. Teukolsky, W. T. Vetterling, and B. P. Flannery, *Numerical Recipes in Fortran 77: The Art of Scientific Computing*, 2nd ed. (Cambridge Univ. Press, New York, 1992).
13. J. Rappaz, Approximation of the spectrum of a non-compact operator given by the magnetohydrodynamic stability of a plasma, *Numer. Math.* **28**, 15 (1977).
14. A. W. Snyder and J. D. Love, *Optical Waveguide Theory* (Chapman–Hall, London, 1983).